Influence of Au and Cu overlayers on the magnetic structure of Co films on W(110)

Thomas Duden and Ernst Bauer
Department of Physics and Astronomy, Arizona State University, Tempe, Arizona 85287-1504
(Received 1 July 1998)

The dependence of the angular distribution of the magnetization in ultrathin epitaxial Co layers upon the thickness of Au and Cu overlayers is studied *in situ* by spin-polarized low-energy electron microscopy in the thickness range from 0 to 3 monolayers. Only Cu overlayers cause a peak in the coverage dependence of the perpendicular magnetic anisotropy at 1.5 ML coverage. The relation between the nanostructure of the overlayers and the anisotropy is discussed. [S0163-1829(99)01501-5]

I. INTRODUCTION

Ultrathin magnetic layer systems with perpendicular magnetic anisotropy (MA) are currently the subject of intensive investigation because of their interesting physics and their application in magnetic storage media and in giant magnetoresistance sensors. Recent work has shown that very low coverages of nonmagnetic materials on top of a magnetic layer can have a strong effect on the direction of the magnetization **M**, as illustrated most dramatically by the 90° in-plane rotation of **M** induced by 0.03 ML Cu on a 7 ML thick Co film on a stepped Cu(001) surface.[1] That the magnetic properties of ultrathin films can be modified by very thin nonmagnetic overlayers has been known for some time[2–4] but only recently it was discovered that they do not change monotonically with overlayer thickness. Polar Kerr effect hysteresis loop studies of ultrathin Co films on Pd(111), Au(111), and Cu(111) substrates showed that deposition of Pd, Cu, Ag or Au lead to a peak in the magnetic anisotropy (MA) just below one monolayer coverage.[5–8] Cu had the most pronounced effect followed by Au, Ag, and Pd. Reflection high-energy electron diffraction[7] and low-energy electron diffraction (LEED) $I(V)$ measurements[9] were used to exclude strain-induced magnetoelastic effects as a possible cause. In other polar Kerr effect hysteresis loop studies of Co layers on Au(111) substrates[10,11] the MA peaks caused by Au and Cu overlayers were observed at 1 and 1.5 ML, respectively, while the value at 1 ML Pd was only slightly above the asymptotic values for thick overlayers. Torsion oscillation magnetometry of Ag and Pd overlayers on Co films on W(110) gave a monotonic change of the anisotropy field and of the second- and fourth-order surface anisotropies derived from it, while Ag produced an extremum of these quantities at 1 ML Ag,[12] and Au overlayers caused an extremum around 0.6–0.7 ML, depending upon the deposition mode.[13] A comparison of the numbers shows that there are considerable differences between the results obtained by different groups.

All these results were obtained by macroscopic, that is laterally averaging methods, in external fields. Recent work has shown[14] that the application of an external field transforms the magnetic microstructure into a metastable single-domain state which cannot be changed into the virginlike state by demagnetization but only by heating. Overlayers generally do not grow monolayer-by-monolayer but consist of regions differing in thickness by as many as three or more monolayers—depending upon thickness—whose individual contributions to the MA cannot be extracted due to the lateral averaging. Clearly, for a basic understanding of the nonmonotonic change of the MA with overlayer coverage a method is needed which does not require the application of external fields and which allows to determine the magnetization and thickness distribution in the film with high lateral resolution. Such a method is spin-polarized low-energy electron microscopy[15] (SPLEEM) with polarization manipulation.[16] It combines magnetic and various topographic contrast modes which are sensitive to monatomic steps and thickness differences on an atomic level with structural information provided by LEED. This allows detailed monitoring of the film growth with a lateral resolution of 10–20 nm as well as the determination of the angular magnetization distribution with a lateral resolution of 20–50 nm. Co layers on W(110) have a strong in-plane anisotropy with a [1-10] easy axis and a perpendicular magnetization component which causes a magnetization wrinkle, that is a spatially fluctuating canting of the magnetization direction out of the film plane.[17] Any increase of the perpendicular anisotropy caused by a nonmagnetic overlayer should tilt the magnetization direction more away from the film plane. Magnetization tilt angle variations due to local overlayer thickness variations will cause corresponding signal variations in the SPLEEM image. This fact is used in the present work to study the dependence of the tilt angle on the thickness and size of regions of constant thickness and to determine the influence of thickness variations on the average tilt angle.

II. EXPERIMENTAL

The experiments were performed in the original LEEM instrument described in Ref. 18 in which the field emission illumination system was replaced by a spin-polarized illumination system with polarization manipulation.[19] An electrostatic objective lens and large Helmholtz coils provide zero magnetic field conditions at the specimen. Imaging in a magnetic field perpendicular to the surface is, in principle, also possible, but fields parallel to the surface cannot be applied during imaging. The base pressure of the instrument was 2×10^{-10} Torr. During the depositions the pressure stayed in the 10^{-10} Torr range and was typically about 6×10^{-10} Torr. The W(110) crystal could be heated from the

backside by radiation up to 500 K and by electron bombardment up to 2000 K. It was precleaned by heating for several hours in the low 10^{-6} Torr range in oxygen and flashing off the oxygen layer in UHV. Between experiments it was cleaned regularly by annealing at approximately 1400 K in 5×10^{-7} Torr oxygen for 30 min, followed by flashing to 2000 K in UHV. Criteria for a clean surface were (i) the absence of W carbide segregation at surface imperfections upon annealing at about 1300 K and (ii) step-flow growth of the first Co monolayer during deposition at 750 K. This growth pattern is very sensitive to surface contamination by segregated or adsorbed impurities which cause pinning of the growth fronts and nucleation on the terraces.

The first monolayer is, therefore, deposited at 750 K. It is filled in two steps: initially a pseudomorphic (ps) monolayer is formed in which close-packed (cp) islands nucleate and grow until the cp monolayer is completed. The completion of the ps and the cp monolayer provides a precise rate calibration before every experiment. After completion of the cp monolayer the sample is allowed to cool to 400 K which takes about 5 min and the deposition is continued to the desired thickness (3–8 ML) at 400 K. At this temperature the mobility is high enough and the two-dimensional nucleation rate low enough so that large terraces (about $300\times300\,\mathrm{nm}^2$) form which show a pronounced thickness-dependent quantum size contrast. This allows the correlation between local magnetization direction and Co film thickness. Once the desired Co film thickness was reached Au or Cu was deposited in doses of 1/8 ML to a total thickness of 3 ML. In the Au overlayer experiments the dependence of the **M** distribution upon the Co thickness temperature was studied. The Au overlayers were deposited at about 400 K in all experiments shown here. In the Cu overlayer experiments, the influence of the morphology of the Cu film on the **M** distribution for Co films of constant thickness (5 ML) was studied. The morphology of the Cu overlayers was changed by preparing them at four different temperatures: (i) close to room temperature in order to decrease mobility and increase nucleation density and (ii) at about 355, 365, and 430 K in order to obtain large terraces and optimum filling of the first overlayer before considerable nucleation and growth occurred in the subsequent overlayer levels. The Au and Cu deposition rates were also calibrated by LEEM before the Co deposition by the time needed to form 1 ML. Typical rates were 1/8 ML/min for both materials.

The images were acquired from the final screen using a CCD camera. For each magnetic image two images resulting from the average of 64 consecutive video frames were taken and stored on disk. Between each single image the polarization vector of the incident beam was inverted by switching the laser helicity of the cathode illumination with a pockels cell. The magnetic signal component was subsequently obtained by performing a normalized subtraction using the formula

$$A=127+100\times K\times(I_+-I_-)/(I_++I_-), \qquad (1)$$

where A is the normalized asymmetry, K is a contrast enhancement factor ranging from 7 to 15 and I_+,I_- are the intensities of the images with opposite spin polarization. In order to reduce noise—which is necessary for a quantitative determination of the **M** distribution—the asymmetry images were low-pass filtered by averaging nonrecursively over 3×3 pixel patches. The average of each patch is stored at the central pixel of the processed image.

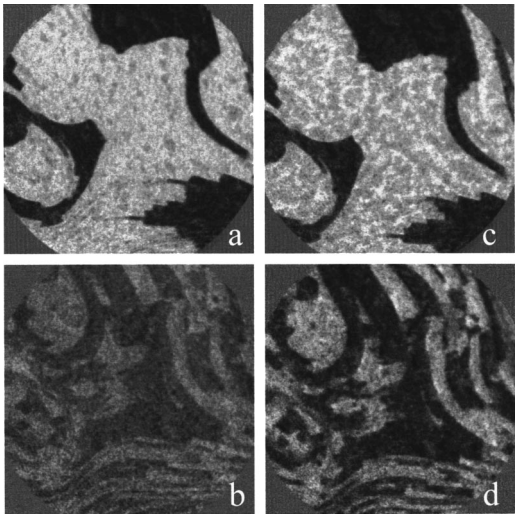

FIG. 1. Magnetic images acquired in the in-plane (a,c) and out-of-plane (b,d) direction. Energy 1.2 eV, field of view ≈7 μm diameter. $K=7$ (a), 15 (b), 8 (c), 10 (d).

III. RESULTS

A. Au overlayers

Figure 1 shows two typical SPLEEM image pairs from a 6 ML thick Co layer, one before Au deposition (a,b) the other after deposition of 1.5 ML Au (c,d), taken with the polarization **P** of the incident beam parallel to the easy in-plane component of **M** (a,c) and to the film normal (b,d). The larger contrast in (d) clearly shows that (a) **M** is tilted more out of the surface plane and (b) the domain size and shape does not change with Au coverage. The distribution of the two grey levels in the bright domain in (c) suggests that the Au layer grows in large double layer islands, a suggestion which is supported by the evolution of the darker regions with Au coverage (not shown). The evolution of the angular **M** distribution with increasing Au coverage was computed from the low-pass filtered **M** component images taken with $\mathbf{P}\parallel\mathrm{W}[1\text{-}10]$ [Figs. 1(a), 1(c), A_0] and $\mathbf{P}\parallel\mathrm{W}[110]$ [Figs. 1(b), 1(d), $A_\perp$] because no magnetic contrast occurs with $\mathbf{P}\parallel\mathrm{W}[001]$ due to the large in-plane anisotropy with the easy axis in the W [1-10] direction. It is then straightforward to compute the tilt angle pixelwise using the formula

$$\alpha=127/(\pi/2)\times\arctan\{(A_0-127)/(A_\perp-127)\}. \qquad (2)$$

The images obtained in this manner give the spatially resolved distribution of the angles between **M** and the specimen surface. The histograms taken from these angular **M** maps are shown in Fig. 2 for two different Co film thicknesses. The bottom curve is from the uncovered Co film and presents the magnetization wrinkle described in Ref. 14. With increasing Au coverage the maxima of the **M** distribution shift to larger angles and become less pronounced. The maxima of the **M** distributions were determined more precisely by fitting the curves shown in Fig. 2 with Gaussians. It is evident that two Gaussians are insufficient. For the mod-

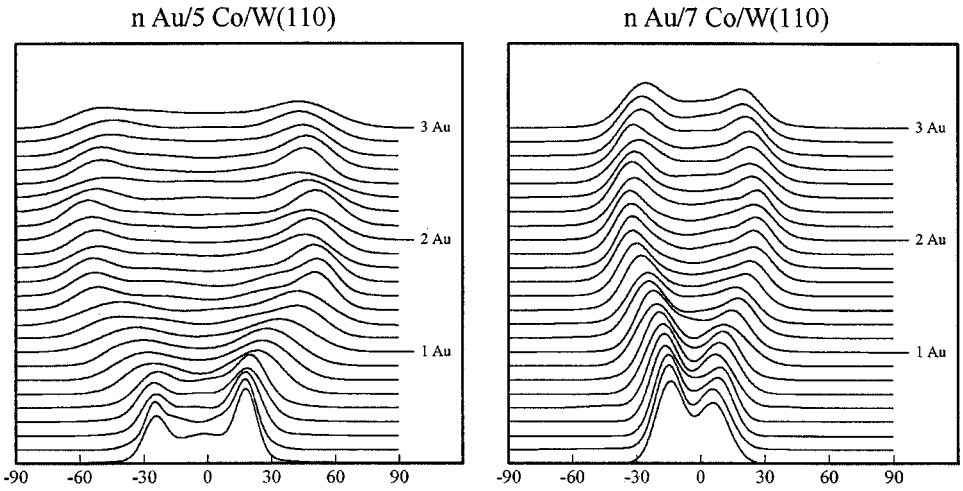

FIG. 2. Histograms taken from the angular distribution maps for different Au coverages. The slight asymmetry in these diagrams was caused by a misalignment of the polarization manipulator which was corrected lateron.

eling of the background noise, one or two additional broader Gaussians centered at or near zero were used which are typically smaller by a factor of 2–3. The angle positions of the strongest Gaussians obtained in this fit are plotted in Fig. 3 for all Co film thicknesses studied. All data except those for seven and eight monolayers have been reproduced at least once. It is apparent that there is no peak at 1 ML but only a slight decrease of the tilt angle in films thicker than 2 ML's which appears to be systematic in spite of the large error bar. At no Co thickness and Au coverage is complete perpendicular magnetization reached.

B. Cu overlayers

The influence of Cu overlayers was studied only for one Co film thickness (5 ML), both for films on W(110) and on 2 ML Cu on W(110). In the case of Co on 2 ML Cu/W(110) no out-of-plane component of the magnetization was found neither in the uncovered Co film nor at any Cu overlayer thickness. The deposition of Cu on Co/W(110), however, caused strong changes of the angular distribution of **M**. Figure 4, in which the experimental data are compiled using the data analysis procedure described above, shows pronounced peaks of the positions of the strongest Gaussians. The four curves were obtained using the specimen temperatures for the growth of the Co film and of the overlayer shown in the diagram. The shape of the curves as well as the position of the maximum depends clearly on the growth temperature. The topographic images show the influence of the deposition temperature on the growth of the Cu overlayer (Fig. 5). At all temperatures studied, Cu growth started with the formation of a first monolayer which grows to approximate completion before the next level becomes visible. This next layer level approached completion after approximately two *additional* monolayers had been deposited, thus leading to the conclusion that second and third layer level grow simultaneously as double layer islands. Due to the higher Cu mobility at elevated specimen temperatures fewer islands with larger extension form in both the first monolayer and the subsequent

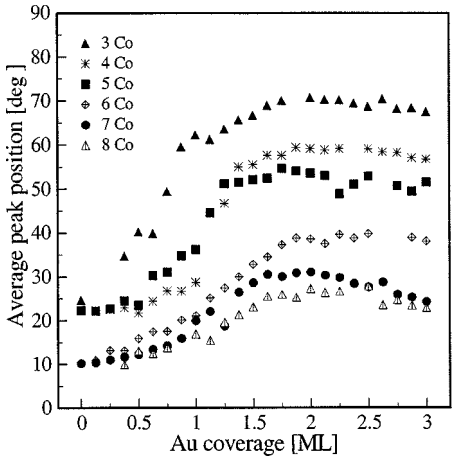

FIG. 3. Positions of the strongest Gaussians compiled from all Au overlayer experiments as a function of Au coverage. Each graph represents all values obtained from one (7,8 ML) or two (3–6 ML) experiments.

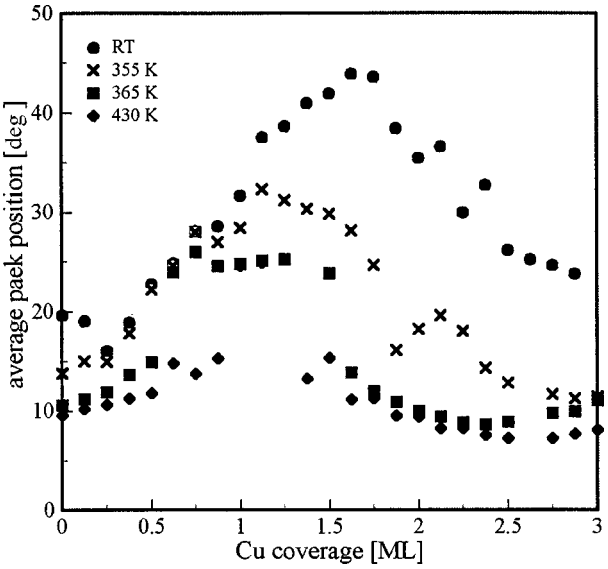

FIG. 4. Positions of the strongest Gaussians as a function of Cu coverage of 5 ML Co on W (110) at four different deposition temperatures.

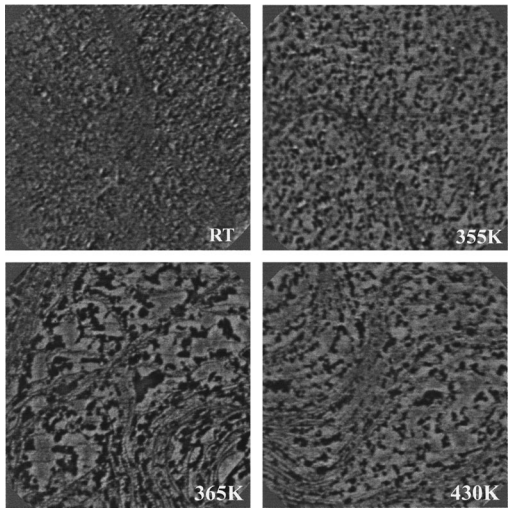

FIG. 5. Topographic images of 1.5 ML Cu grown on 5 ML Co on W(110) at different temperatures, $E=1.4$ eV, field of view $\approx 7 \times 7\ \mu m^2$. The temperature at which the last Co layer and the Cu layers were deposited is shown.

double layer as illustrated in Fig. 5. The higher temperatures also lead to a more perfect filling of the first monolayer.

The large islands obtained at elevated growth temperatures allow a layer-level specific evaluation of the angular magnetization distribution, thus enabling a more detailed study of how regions with different overlayer thickness contribute to the **M** tilt. Figure 6 shows the evolution of the tilt distribution in the different regions during the 365 K deposition. The open triangles represent the tilt in the regions without Cu coverage, the solid spheres give the tilt in the regions covered with 1 ML Cu and the open squares show the data collected from the areas covered with 3 ML Cu (monolayer+double layer islands). It is obvious that only regions with 1 ML Cu coverage contribute to the extremal tilt of the magnetization whereas the tilt directions in the other areas remain unchanged within the limits of error.

The clear correlation between layer levels and tilt angle distribution explains the shape of the overall peak position curve in Fig. 4: At first, 1 ML thick Cu islands grow at the expense of the uncovered regions causing the overall increase of the tilt angle. Saturation is reached when the first monolayer level is dominating. The double-layer islands of the second and third overlayer levels begin to grow while the residual uncovered regions vanish. When the double layer islands start to grow at the expense of the 1 ML level, the splitting decreases rapidly and converges to its final value at 3 complete ML's. The largest tilts are obtained during growth near room temperature (Fig. 4). Apparently, other factors in addition to hybridization in the first monolayer, such as particle size-dependent strain play a role too. The fine grained structure of the Cu islands (Fig. 5) does, however, not allow the analysis carried out for the lower temperatures. Only for Cu coverages above 1.5 ML is a distinction between the $0+1$ ML levels and the 3 ML level possible in this case, but the clear correlation between layer levels and tilt angle is lost.

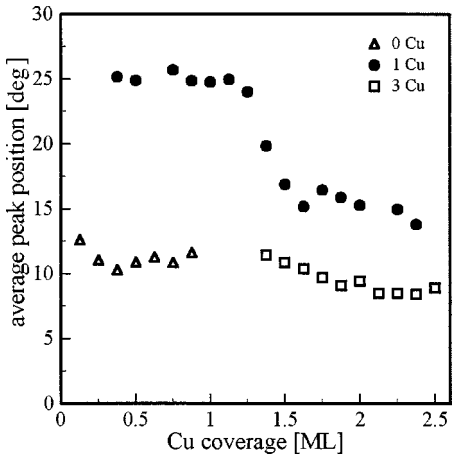

FIG. 6. Local overlayer thickness-dependent evaluation of the magnetization tilt angle for the 365 K deposition of Cu on 5 ML Co on W(110).

IV. DISCUSSION

In the Au/Co/W(110) experiments the magnetization tilt develops nearly monotonically and approaches its final value at about 2 ML Au with no apparent peak. The double-layer growth indicated by the quantum size contrast in Fig. 1(c) and supported by theoretical considerations[20] is a straightforward explanation of the absence of a peak at lower Au coverages. The observation of a peak at 0.6–0.7 ML,[13] slightly below 1 ML,[7,8] or at 1 ML (Refs. 10, 11) in earlier studies in which the films were grown at lower temperatures would then imply initial monolayer growth up to 0.6–0.7 ML or up to about 1 ML at the lower growth temperatures. First-principles calculations for a pseudomorphic Co ML on Au(111) (Ref. 21) give also a peak at 1 ML Au. The electronic structure of this loosely packed Co ML is certainly very different from that of the close-packed Co layer studied in the experiments—the packing ratio is 0.75:1—so that it is difficult to compare theory and experiment.

The layer level-resolved analysis of the Cu/Co/W(110) images clearly establish a correlation between the maximum magnetization tilt angle regions and the 1 ML Cu level at the higher growth temperatures. This is in qualitative agreement with first-principles calculations for a pseudomorphic Co ML on Cu(111) which predicts a switch from the in-plane anisotropy of the uncovered Co ML to perpendicular anisotropy only for a 1 ML thick Cu overlayer while 2 ML Cu produces a slight in-plane anisotropy again.[22] At deposition temperatures closer to RT, however, the maximum tilt of **M** occurs at higher Cu coverages (1.5 ML) indicating a delayed completion of the 1 ML Cu level combined with an increase of the overall anisotropy probably caused by strain exerted by the double-layer islands. This conjecture is supported by a very recent study of the early stages of growth of Cu on the (0001) surface of bulk Co at room temperature by scanning tunneling microscopy and LEED.[23] At 1.25 ML Cu the first ML covered 60% and the second ML 30% of the surface, while 5% were still uncovered and the other 5% was occupied by three-dimensional crystals. The LEED results of this work show that above 1.25 ML the Cu layer induces stacking-faulted regions in the top Co layer which extend over the complete surface at 2.7 ML Cu. This structural rearrangement in the topmost Co layer is a possible cause of

the decrease of the perpendicular anisotropy beyond the peak.

The tilt angle $\alpha = 1 - \theta$ is determined by the minimum of the total energy $E(\theta)$ which in the absence of an external field gives[17]

$$\sin^2 \theta = \frac{2\pi M_s^2 - K_{1b} - K_{1s}/t}{2K_{2b} + 2K_{2s}/t}. \quad (3)$$

Here M_s is the saturation magnetization and the K_{ik} are the second- $(i=1)$ and fourth- $(i=2)$ order anisotropy coefficients which are proportional to the thickness (''bulk'' anisotropies, $k=b$) or are independent of t (''surface'' anisotropies, $k=s$). At fixed t, M_s, K_{1b}, and K_{2b} may be assumed to be independent of overlayer coverage, at least if it does not introduce a significant amount of strain. Then the changes of the tilt angle with overlayer coverage must be caused by changes of K_{1s} and/or K_{2s}. The striking increase of α (decrease of θ) caused by 1 ML Cu (Fig. 6) and its decrease at 3 ML Cu to its value at the uncovered surface may then be attributed to the hybridization between Co and Cu electrons in the wetting monolayer and the subsequent dehybridization once the Cu layer develops the bulk electronic structure. This is a very general phenomenon in strongly interacting film systems as illustrated, for example, by the system Co/W(110) (Ref. 24) and reviewed recently.[25] The same explanation is suggested for the absence of a peak of the tilt angle in the present Au/Co study at elevated deposition temperatures at which a double layer forms initially in contrast to the monolayer growth in earlier work at room temperature in which a peak was observed. The dependence of the tilt angle upon the thickness t of the Co layer (Fig. 3) follows immediately from Eq. (3), with correspondingly larger K_{1s}, K_{2s} values than in the case of uncovered Co layers.[17] The temperature dependence of the tilt angle (Fig. 4) is mainly due to structural differences but a temperature dependence of the anisotropy coefficients as in Co/Pt layers,[26] for example, cannot be excluded.

Both overlayer experiments and the comparison with previous overlayer studies clearly show the strong influence of the nanostructure of the overlayers on their magnetic properties. They suggest that the appearance of a peak in the perpendicular magnetic anisotropy depends upon the structure of the overlayer and that the differences between different studies are due to differences in the growth mode which depends strongly upon the deposition conditions. The present study does not support, however, the recent suggestion[26] that Au overlayers cause a drastic smoothing of the Co free surface and an increase of the magnetic domain size.

V. CONCLUSIONS

It is evident that the deposition conditions are of crucial importance for the evolution of the magnetic structure of thin ferromagnetic films with the thickness of nonmagnetic overlayers. So far, only SPLEEM allows us to investigate the correlation between structure and magnetism as illustrated in this article. The discrepancies between published results of the influence of overlayers are easily explained by the high sensitivity of the structure of the overlayer to the deposition temperature and by the averaging over several layer levels in all past experiments which lack the lateral resolution necessary for an unambiguous connection between overlayer thickness and **M** orientation.

ACKNOWLEDGMENTS

The authors wish to thank the TU Clausthal for the loan of the SPLEEM equipment.

[1] W. Weber, C. H. Back, A. Bischof, D. Pescia, and R. Allenspach, Nature (London) **374**, 888 (1995).
[2] E. Bergter, U. Gradmann, and R. Bergholz, Solid State Commun. **53**, 565 (1985).
[3] H.-J. Elmers and U. Gradmann, Surf. Sci. **193**, 94 (1988).
[4] W. Weber, D. Kerkmann, D. Pescia, D. A. Wesner, and G. Guentherodt, Phys. Rev. Lett. **65**, 2058 (1990).
[5] B. N. Engel, M. H. Wiedmann, R. A. Van Leeuwen, and C. M. Falco, Phys. Rev. B **48**, 9894 (1993); J. Appl. Phys. **73**, 6192 (1993).
[6] M. H. Wiedmann, B. N. Engel, R. A. Van Leeuwen, K. Mibu, T. Shinjo, and C. M. Falco, in *Magnetic Ultrathin Films, Multilayers and Surfaces/Interfaces and Characterization*, edited by B. T. Jonker *et al.*, MRS Symposia Proceedings No. 313 (Materials Research Society, Pittsburgh, 1993) p. 531.
[7] B. N. Engel, M. H. Wiedmann, and C. M. Falco, J. Appl. Phys. **75**, 6401 (1994).
[8] M. H. Wiedmann, C. Marliere, B. N. Engel, and C. M. Falco, J. Magn. Magn. Mater. **148**, 125 (1995).
[9] M. H. Wiedmann, B. N. Engel, and C. M. Falco, J. Appl. Phys. **76**, 6075 (1994).
[10] S. Ould-Mahfoud, R. Mégy, N. Bardou, B. Bartelian, P. Beauvillain, C. Chappert, J. Corno, B. Lecuyer, G. Sczigel, P. Veillet, and D. Weller, in *Magnetic Ultrathin Films, Multilayers and Surfaces/Interfaces and Characterization* (Ref. 6), p. 251.
[11] P. Beauvillain, A. Bournouh, C. Chappert, R. Mégy, S. Ould-Mahfoud, J. R. Renard, P. Veillet, D. Weller, and J. Corno, J. Appl. Phys. **76**, 6078 (1994).
[12] J. Kohlhepp and U. Gradmann, J. Magn. Magn. Mater. **139**, 347 (1995).
[13] H. Fritzsche, J. Kohlhepp, and U. Gradmann, J. Magn. Magn. Mater. **148**, 154 (1995).
[14] M. Speckmann, H. P. Oepen, and H. Ibach, Phys. Rev. Lett. **75**, 2035 (1995).
[15] E. Bauer, in *Handbook of Microscopy*, edited by S. Amelynckx, D. van Dyck, L. van Landuyt, and G. van Tendeloo (VCH, New York, 1997), p. 751.
[16] T. Duden and E. Bauer, Rev. Sci. Instrum. **66**, 2861 (1995).
[17] T. Duden and E. Bauer, Phys. Rev. Lett. **77**, 2308 (1996).
[18] E. Bauer and W. Telieps, in *Surface and Interface Characterization by Electron Optical Methods*, edited by A. Horne and U. Valdré (Plenum, New York, 1988).
[19] T. Duden, Ph.D. thesis, TU Clausthal, 1996; see also Fig. 3 in Ref. 15.
[20] J. H. van der Merwe and E. Bauer, Phys. Rev. B **39**, 3632 (1989).
[21] B. Ujfalussy, L. Szunyogh, P. Bruno, and P. Weinberger, Phys. Rev. Lett. **77**, 1805 (1996).

[22] L. Zhong, M. Kim, X. Wang, and A. J. Freeman, Phys. Rev. B **53**, 9770 (1996).
[23] J. E. Prieto, Ch. Rath, S. Mueller, R. Miranda, and K. Heinz, Surf. Sci. **401**, 248 (1998).
[24] H. Knoppe and E. Bauer, Phys. Rev. B **48**, 1794 (1993).
[25] F. J. Himpsel, J. E. Ortega, G. J. Mankey, and R. F. Willis, Adv. Phys. **47**, 511 (1998).
[26] J. Ferre, J. P. Jamet, J. Pommier, P. Beauvillain, C. Chappert, R. Megy, and P. Veillet, J. Magn. Magn. Mater. **174**, 77 (1997).